On the Analysis and Design of Spurline Bandstop Filters

CAM NGUYEN, MEMBER, IEEE, AND KAI CHANG, SENIOR MEMBER, IEEE

Abstract —**The parameters of general two-coupled lines and symmetric three-coupled lines in an inhomogeneous medium for the lossless case are obtained. The impedance and chain matrices of spurline bandstop filters are derived. One-section spurline bandstop filters with their stopbands centered near 33 GHz have been designed and tested. There is excellent agreement between the experimental results and those predicted theoretically.**

I. Introduction

RECENT ADVANCES in microwave and milimeter-wave integrated circuits have created a demand for compact bandstop filters; spurline bandstop filters (Fig. 1) are most promising. They are compact structures, with a significantly lower radiation loss than conventional shunt-stub and coupled-line filters [1].

A basic spurline bandstop filter, consisting of two identical parallel conductors (Fig. 1(a)) built in stripline configuration, was first introduced by Schiffman and Matthaei [2]. Bates adapted this technique in microstrip medium by assuming the same phase velocities for even and odd modes [1]. Later, Nguyen *et al.* analyzed the structure, taking into account the different even- and odd-mode phase velocities [3]. None of the papers published on this subject, however, analyze spurline filters using asymmetrical two lines (Fig. 1(b)) and symmetrical three lines (Fig. 1(c)).

The principal advantages of the asymmetric two-line filter are its ability to act as a symmetrical two-line filter combined with an impedance transformer, and can be designed to achieve a wider stop-bandwidth by choosing appropriate dimensions for the asymmetric coupled lines. The symmetrical three-line filter has significant advantages over asymmetrical and symmetrical two-line filters because it can offer a much wider bandwidth in addition to a higher stopband rejection in a comparable size.

It is the intent of this paper to provide an analysis and performance of such spurline bandstop filters in an inhomogeneous medium.

To study the theoretical behavior of spurline networks, the parameters of the corresponding lossless coupled lines are also obtained completely in terms of the static capacitance matrix for the structure and the capacitance matrix of the same structure with the dielectric removed.

II. General Two-Coupled Lines

Fig. 2 shows a nonidentical, coupled transmission line embedded in an inhomogeneous medium. This structure supports two quasi-TEM propagation modes, designated here as mode C and mode π.

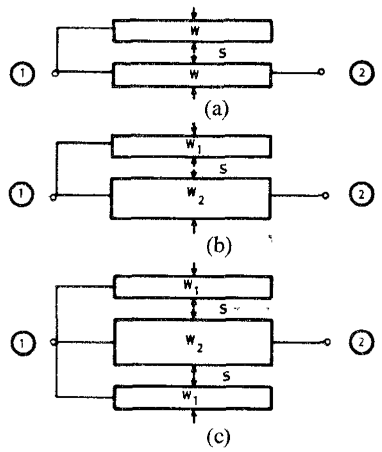

Fig. 1. Spurline bandstop filter configurations.

The propagation constants and ratios of voltages $R_{C,\pi}$ on the lines for the two modes have been obtained in terms of the elements of the per-unit-length inductance and capacitance matrices of the structure [4]. Assuming the dielectric is nonmagnetic, the two distinct velocities $v_{C,\pi}$ and parameters $R_{C,\pi}$ for the two modes can now be derived in terms of the elements of the per-unit-length capacitance matrices of the structure with and without the presence of the dielectric, C_{ij} and C_{0ij} $(i, j = 1,2)$, respectively. They are given as follows:

$$v_{C,\pi} = \left\{ \frac{D_1 + D_2}{2} \pm \frac{1}{2}\left[(D_1 - D_2)^2 + 4E_1E_2 \right]^{1/2} \right\}^{-1/2} \tag{1}$$

and

$$R_{C,\pi} = \frac{1}{2E_1}\left\{ (D_2 - D_1) \pm \left[(D_2 - D_1)^2 + 4E_1E_2 \right]^{1/2} \right\} \tag{2}$$

where

$$\begin{aligned} D_1 &= (C_{11}C_{022} - C_{12}C_{012})/(v_0^2 \cdot \det[C_0]) \\ D_2 &= (C_{22}C_{011} - C_{12}C_{012})/(v_0^2 \cdot \det[C_0]) \\ E_1 &= (C_{12}C_{022} - C_{22}C_{012})/(v_0^2 \cdot \det[C_0]) \\ E_2 &= (C_{12}C_{011} - C_{11}C_{012})/(v_0^2 \cdot \det[C_0]) \end{aligned} \tag{3}$$

with

$$\det[C_0] = C_{011}C_{022} - C_{012}^2. \tag{4}$$

Manuscript received March 15, 1985; revised June 25, 1985.
The authors are with TRW, One Space Park, Redondo Beach, CA 90278.

0018-9480/85/1200-1416$01.00 ©1985 IEEE

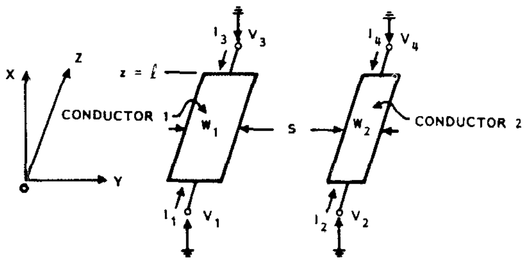

Fig. 2. Schematic of a pair of coupled lines with unequal width.

v_0 is the free-space velocity. The characteristic impedance Z_{0ik} ($i=1,2$ and $k=C,\pi$) of line i for mode k can be derived as

$$Z_{01k}=\frac{1}{v_k(C_{11}+R_kC_{12})}=\frac{1}{Y_{01k}} \tag{5a}$$

$$Z_{02k}=\frac{1}{v_k(C_{22}+R_k^{-1}C_{12})}=\frac{1}{Y_{02k}}. \tag{5b}$$

The total static capacitance per unit length C_{ik} of line i for mode k, thus, can be seen to be

$$C_{1k}=C_{11}+R_kC_{12} \tag{6a}$$

$$C_{2k}=C_{22}+R_k^{-1}C_{12}. \tag{6b}$$

The elements of the impedance and admittance matrices have been obtained for a general case in [5]. For a lossless coupled lines structure, they can be found to be

$$Z_{11}=Z_{33}=-j\left[\frac{Z_{01C}\cot\theta_C}{(1-R_C/R_\pi)}+\frac{Z_{01\pi}\cot\theta_\pi}{(1-R_\pi/R_C)}\right]$$

$$Z_{12}=Z_{21}=Z_{34}=Z_{43}$$

$$=-j\left[\frac{Z_{01C}R_C\cot\theta_C}{(1-R_C/R_\pi)}+\frac{Z_{01\pi}R_\pi\cot\theta_\pi}{(1-R_\pi/R_C)}\right]$$

$$=j\left[\frac{Z_{02C}\cot\theta_C}{R_\pi(1-R_C/R_\pi)}+\frac{Z_{02\pi}\cot\theta_\pi}{R_C(1-R_\pi/R_C)}\right]$$

$$Z_{14}=Z_{41}=Z_{23}=Z_{32}$$

$$=-j\left[\frac{R_CZ_{01C}}{(1-R_C/R_\pi)\sin\theta_C}+\frac{R_\pi Z_{01\pi}}{(1-R_\pi/R_C)\sin\theta_\pi}\right]$$

$$Z_{13}=Z_{31}$$

$$=-j\left[\frac{Z_{01C}}{(1-R_C/R_\pi)\sin\theta_C}+\frac{Z_{01\pi}}{(1-R_\pi/R_C)\sin\theta_\pi}\right]$$

$$Z_{22}=Z_{44}=j\left[\frac{R_CZ_{02C}\cot\theta_C}{R_\pi(1-R_C/R_\pi)}+\frac{R_\pi Z_{02\pi}\cot\theta_\pi}{R_C(1-R_\pi/R_C)}\right]$$

$$=-j\left[\frac{R_C^2Z_{01C}\cot\theta_C}{(1-R_C/R_\pi)}+\frac{R_\pi^2Z_{01\pi}\cot\theta_\pi}{(1-R_\pi/R_C)}\right]$$

$$Z_{24}=Z_{42}$$

$$=-j\left[\frac{R_C^2Z_{01C}}{(1-R_C/R_\pi)\sin\theta_C}+\frac{R_\pi^2Z_{01\pi}}{(1-R_\pi/R_C)\sin\theta_\pi}\right] \tag{7}$$

and

$$Y_{11}=Y_{33}=-j\frac{Y_{01C}\cot\theta_C}{(1-R_C/R_\pi)}+\frac{Y_{01\pi}\cot\theta_\pi}{(1-R_\pi/R_C)}$$

$$Y_{12}=Y_{21}=Y_{34}=Y_{43}$$

$$=j\left[\frac{Y_{01C}\cot\theta_C}{R_\pi(1-R_C/R_\pi)}+\frac{Y_{01\pi}\cot\theta_\pi}{R_C(1-R_\pi/R_C)}\right]$$

$$Y_{14}=Y_{41}=Y_{23}=Y_{32}$$

$$=-j\left[\frac{Y_{01C}}{(R_\pi-R_C)\sin\theta_C}+\frac{Y_{01\pi}}{(R_C-R_\pi)\sin\theta_\pi}\right]$$

$$Y_{13}=Y_{31}=j\left[\frac{Y_{01C}}{(1-R_C/R_\pi)\sin\theta_C}+\frac{Y_{01\pi}}{(1-R_\pi/R_C)\sin\theta_\pi}\right]$$

$$Y_{22}=Y_{44}=+j\left[\frac{R_CY_{02C}\cot\theta_C}{R_\pi(1-R_C/R_\pi)}+\frac{R_\pi Y_{02\pi}\cot\theta_\pi}{R_C(1-R_\pi/R_C)}\right]$$

$$Y_{24}=Y_{42}=-j\left[\frac{R_CY_{02C}}{R_\pi(1-R_C/R_\pi)\sin\theta_C}+\frac{R_\pi Y_{02\pi}}{R_C(1-R_\pi/R_C)\sin\theta_\pi}\right] \tag{8}$$

where $\theta_{C,\pi}$ are the electrical lengths of the line for the two modes. For the special case of two symmetrical coupled lines, the two propagation modes become an even mode and an odd mode. The even- and odd-mode phase velocities are obtained as

$$v_{pe,o}=v_0\left[\frac{C_{011}\pm C_{012}}{C_{11}\pm C_{12}}\right]^{1/2} \tag{9}$$

where the subscripts e and o denote even and odd modes, respectively, and the even- and odd-mode characteristic impedances are

$$Z_{0e}=\frac{1}{v_{pe}(C_{11}+C_{12})} \tag{10a}$$

$$Z_{0o}=\frac{1}{v_{po}(C_{11}-C_{12})} \tag{10b}$$

whereas

$$C_{0e,o}=C_{11}\pm C_{12} \tag{11}$$

are the even- and odd-mode static capacitance per unit length.

III. Symmetric Three-Coupled Lines

In the structure of three symmetric coupled lossless lines in an inhomogeneous medium (Fig. 3), there are three quasi-TEM propagation modes, referred to here as modes a, b, and c.

The propagation constants and ratios of voltages on the lines for the three modes have been characterized in terms of the elements of series impedance and shunt admittance per-unit-length matrices of the structure [6]. In this paper, the distinct phase velocities $v_{a,b,c}$ and ratios of voltages are derived in terms of the elements of the static capacitance matrices C_{ij} and C_{0ij} ($i,j=1,2,3$) of the structure with the dielectric in place and removed, respectively, and are given by

$$\nu_a = (B_1 - B_3)^{-1/2} \tag{12a}$$

$$\nu_{b,c} = \left\{ \frac{B_1 + B_3 + B_5}{2} \pm \frac{1}{2}\left[(B_1 + B_3 - B_5)^2 + 8B_2B_4 \right]^{1/2} \right\}^{-1/2} \tag{12b}$$

and

$$R_{2b,c} = \frac{1}{2B_2}\left\{ -(B_1 + B_3 - B_5) \pm \left[(B_1 + B_3 - B_5)^2 + 8B_2B_4 \right]^{1/2} \right\} \tag{13}$$

where $R_{ik} = V_{ik}/V_{1k}$, $i = 2,3$ and $k = a, b, c$, is defined as the ratio of voltage on the ith to the voltage on the first lines in mode k

$$\begin{aligned} B_1 &= \left[C_{11}(C_{011}C_{022} - C_{012}^2) + C_{12}C_{012}(C_{013} - C_{011}) + C_{13}(C_{012}^2 - C_{013}C_{022}) \right] / \nu_0^2 \cdot \det[C_0] \\ B_2 &= \left[C_{12}(C_{011}C_{022} - C_{012}^2) + C_{22}C_{012}(C_{013} - C_{011}) + C_{12}(C_{012}^2 - C_{013}C_{022}) \right] / \nu_0^2 \cdot \det[C_0] \\ B_3 &= \left[C_{13}(C_{011}C_{022} - C_{012}^2) + C_{12}C_{012}(C_{013} - C_{011}) + C_{11}(C_{012}^2 - C_{013}C_{022}) \right] / \nu_0^2 \cdot \det[C_0] \\ B_4 &= \left[C_{11}C_{012}(C_{013} - C_{011}) + C_{12}(C_{011}^2 - C_{013}^2) + C_{13}C_{012}(C_{013} - C_{011}) \right] / \nu_0^2 \cdot \det[C_0] \\ B_5 &= \left[C_{22}(C_{011}^2 - C_{013}^2) + 2C_{12}C_{012}(C_{013} - C_{011}) \right] / \nu_0^2 \cdot \det[C_0] \end{aligned} \tag{14}$$

with

$$\det[C_0] = [C_{011} - C_{013}]\left[C_{022}(C_{011} + C_{013}) - 2C_{012}^2 \right]. \tag{15}$$

The characteristic impedance and admittance Z_{0ik} and Y_{0ik} ($i = 1,2,3$ and $k = a, b, c$), respectively, of line i for mode k can be derived as follows:

$$Z_{01a} = Z_{03a} = \frac{1}{\nu_a(C_{11} - C_{13})} = \frac{1}{Y_{01a}} = \frac{1}{Y_{03a}} \tag{16a}$$

$$Z_{01b} = Z_{03b} = \frac{1}{\nu_b(C_{11} + R_{2b}C_{12} + C_{13})} = \frac{1}{Y_{01b}} = \frac{1}{Y_{03b}} \tag{16b}$$

$$Z_{02b} = \frac{1}{\nu_b(C_{22} + 2C_{12}/R_{2b})} = \frac{1}{Y_{02b}} \tag{16c}$$

$$Z_{01c} = Z_{03c} = \frac{1}{\nu_c(C_{11} + R_{2c}C_{12} + C_{13})} = \frac{1}{Y_{01c}} = \frac{1}{Y_{03c}} \tag{16d}$$

and

$$Z_{02c} = \frac{1}{\nu_c(C_{22} + 2C_{12}/R_{2c})} = \frac{1}{Y_{02c}}. \tag{16e}$$

The total static capacitance per unit length C_{ik} of line i for mode k, therefore, can be seen to be

$$C_{1a} = C_{3a} = C_{11} - C_{13} \tag{17a}$$

$$C_{1b} = C_{3b} = C_{11} + R_{2b}C_{12} + C_{13} \tag{17b}$$

$$C_{2b} = C_{22} + 2C_{12}/R_{2b} \tag{17c}$$

$$C_{1c} = C_{3c} = C_{11} + R_{2c}C_{12} + C_{13} \tag{17d}$$

$$C_{2c} = C_{22} + 2C_{12}/R_{2c}. \tag{17e}$$

The impedance and admittance matrix parameters have been obtained for a general case in [6]. For a lossless structure, they can be derived as follows:

$$\begin{aligned} Z_{11} &= Z_{33} = Z_{44} = Z_{66} \\ &= -j\tfrac{1}{2}\left[Z_{01a}\cot\theta_a - (R_{2c}Z_{01b}\cot\theta_b - R_{2b}Z_{01c}\cot\theta_c)/R_d \right] \\ Z_{12} &= Z_{21} = Z_{23} = Z_{32} \\ &= Z_{54} = Z_{45} = Z_{56} = Z_{65} \\ &= -j(Z_{02b}\cot\theta_b - Z_{02c}\cot\theta_c)/R_d \\ Z_{13} &= Z_{31} = Z_{46} = Z_{64} \\ &= j\tfrac{1}{2}\left[Z_{01a}\cot\theta_a + (R_{2c}Z_{01b}\cot\theta_b - R_{2b}Z_{01c}\cot\theta_c)/R_d \right] \\ Z_{14} &= Z_{41} = Z_{36} = Z_{63} \\ &= -j\tfrac{1}{2}\left[Z_{01a}\csc\theta_a + (R_{2b}Z_{01c}\csc\theta_c - R_{2c}Z_{01b}\csc\theta_b)/R_d \right] \\ Z_{15} &= Z_{51} = Z_{24} = Z_{42} \\ &= Z_{35} = Z_{53} = Z_{26} = Z_{62} \\ &= -j(Z_{02b}\csc\theta_b - Z_{02c}\csc\theta_c)/R_d \\ Z_{16} &= Z_{61} = Z_{34} = Z_{43} \\ &= j\tfrac{1}{2}\left[Z_{01a}\csc\theta_a + (R_{2c}Z_{01b}\csc\theta_b - R_{2b}Z_{01c}\csc\theta_c)/R_d \right] \\ Z_{22} &= Z_{55} \\ &= -j(R_{2b}Z_{02b}\cot\theta_b - R_{2c}Z_{02c}\cot\theta_c)/R_d \\ Z_{25} &= Z_{52} \\ &= -j(R_{2b}Z_{02b}\csc\theta_b - R_{2c}Z_{02c}\csc\theta_c)/R_d \end{aligned} \tag{18}$$

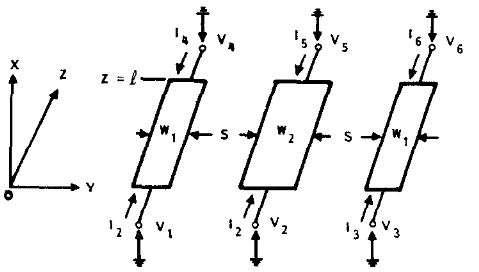

Fig. 3. Schematic of symmetrical three-coupled lines.

and

$$
\begin{aligned}
Y_{11} &= Y_{33} = Y_{44} = Y_{66} \\
&= -j\tfrac{1}{2}\left[Y_{01a}\cot\theta_a - (R_{2c}Y_{01b}\cot\theta_b - R_{2b}Y_{01c}\cot\theta_c)/R_d\right] \\
Y_{12} &= Y_{21} = Y_{23} = Y_{32} \\
&= Y_{45} = Y_{54} = Y_{56} = Y_{65} \\
&= -j(Y_{01b}\cot\theta_b - Y_{01c}\cot\theta_c)/R_d \\
Y_{13} &= Y_{31} = Y_{46} = Y_{64} \\
&= j\tfrac{1}{2}\left[Y_{01a}\cot\theta_a + (R_{2c}Y_{01b}\cot\theta_b - R_{2b}Y_{01c}\cot\theta_c)/R_d\right] \\
Y_{14} &= Y_{41} = Y_{36} = Y_{63} \\
&= j\tfrac{1}{2}\left[Y_{01a}\csc\theta_a + (R_{2b}Y_{01c}\csc\theta_c - R_{2c}Y_{01b}\csc\theta_b)/R_d\right] \\
Y_{15} &= Y_{51} = Y_{24} = Y_{42} \\
&= Y_{35} = Y_{53} = Y_{26} = Y_{62} \\
&= j(Y_{01b}\csc\theta_b - Y_{01c}\csc\theta_c)/R_d \\
Y_{16} &= Y_{61} = Y_{34} = Y_{43} \\
&= -j\tfrac{1}{2}\left[Y_{01a}\csc\theta_a + (R_{2c}Y_{01b}\csc\theta_b - R_{2b}Y_{01c}\csc\theta_c)/R_d\right] \\
Y_{22} &= Y_{55} \\
&= -j(R_{2b}Y_{02b}\cot\theta_b - R_{2c}Y_{02c}\cot\theta_c)/R_d \\
Y_{25} &= Y_{52} \\
&= j(R_{2b}Y_{02b}\csc\theta_b - R_{2c}Y_{02c}\csc\theta_c)/R_d
\end{aligned} \tag{19}
$$

where $\theta_{a,b,c}$ are the electrical lengths of the lines for the three modes, and

$$R_d = R_{2b} - R_{2c}. \tag{20}$$

IV. Spurline Bandstop Filters

A. Two-Conductor Spurline Filter

Fig. 4 shows the schematic of a single section of the spurline bandstop filter employing two coupled lines. After applying the appropriate boundary conditions to the impedance matrix in Section II, the *ABCD* matrix parameters

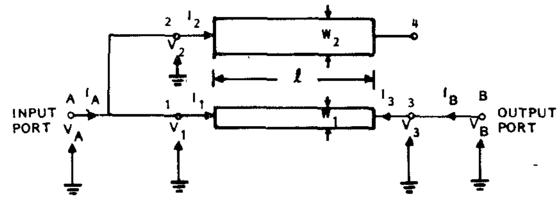

Fig. 4. Schematic of two-conductor spurline section.

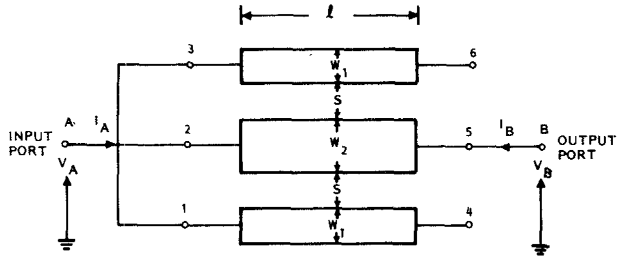

Fig. 5. Schematic of three-conductor spurline section.

of this two-port spurline network can be derived as

$$A = \frac{\cos\theta_C\cos\theta_\pi(R_C - R_\pi)}{R_C(1-R_\pi)\cos\theta_\pi - R_\pi(1-R_C)\cos\theta_C}$$

$$C = \frac{j}{R_C(1-R_\pi)\cos\theta_\pi - R_\pi(1-R_C)\cos\theta_C} \cdot \left[\frac{(1-R_C)^2\cos\theta_C}{R_C Z_{01\pi}\csc\theta_\pi} - \frac{(1-R_\pi)^2\cos\theta_\pi}{R_\pi Z_{01C}\csc\theta_C}\right]$$

$$
\begin{aligned}
D = \Big\{ &\cos\theta_C\cos\theta_\pi\left[R_\pi^2(1-R_C)^2 + R_C^2(1-R_\pi)^2\right] \\
&+ R_C R_\pi \sin\theta_C \sin\theta_\pi \cdot \left[\frac{Z_{01C}}{Z_{01\pi}}(1-R_C)^2 + \frac{Z_{01\pi}}{Z_{01C}}(1-R_\pi)^2\right] \\
&- 2R_C R_\pi(1-R_C)(1-R_\pi)\Big\} \\
&/(R_C - R_\pi)\left[R_C(1-R_\pi)\cos\theta_\pi - R_\pi(1-R_C)\cos\theta_C\right]
\end{aligned}
$$

and

$$B = \frac{1}{C}(AD-1). \tag{21}$$

For the special case of a spurline structure consisting of two identical coupled lines, the above equations reduce to those obtained in [3]. The open-circuit impedance matrix of the spurline network can also be obtained in a similar fashion.

B. Three-Conductor Spurline Filter

A single section of a spurline bandstop filter consisting of three symmetrical coupled lines is illustrated in Fig. 5.

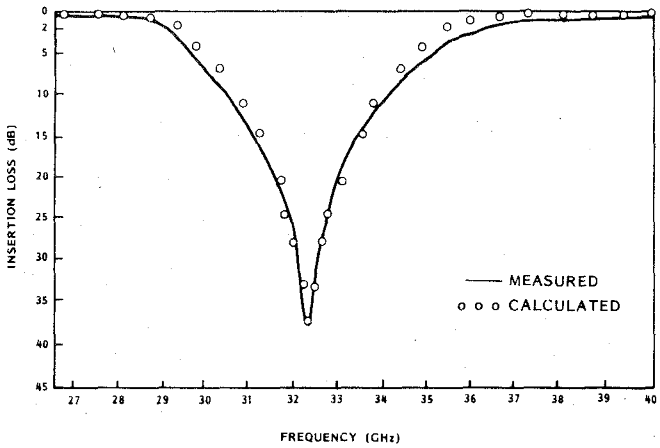

Fig. 6. Transmission loss for single-section two-line spurline filter.

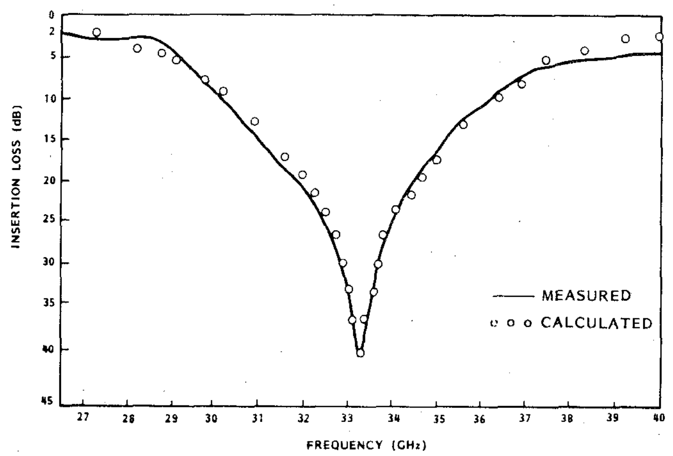

Fig. 7. Transmission loss for single-section three-line spurline filter.

After the appropriate termination conditions are applied to the coupled-line six-port network characterized by an impedance matrix in Section III, the chain matrix and open-circuit impedance matrix of this spurline network can be obtained as

$$\begin{bmatrix} V_A \\ I_A \end{bmatrix} = \frac{1}{M}\begin{bmatrix} L & (LN-M^2)/E \\ E & N \end{bmatrix}\begin{bmatrix} V_B \\ -I_B \end{bmatrix} \tag{22}$$

and

$$\begin{bmatrix} V_A \\ V_B \end{bmatrix} = \frac{1}{E}\begin{bmatrix} L & M \\ M & N \end{bmatrix}\begin{bmatrix} I_A \\ I_B \end{bmatrix} \tag{23}$$

where

$$E = -\frac{2j}{R_d}\Big[Z_{02b}\cot\theta_b(2-R_{2b}) - Z_{02c}\cot\theta_c(2-R_{2c}) + \frac{1}{2}R_{2c}Z_{01b}\cot\theta_b\Big]$$

$$L = -\frac{1}{R_d^2}\big\{2(Z_{02b}\cot\theta_b - Z_{02c}\cot\theta_c)^2 + R_{2c}Z_{01b}\cot\theta_b(R_{2b}Z_{02b}\cot\theta_b - R_{2c}Z_{02c}\cot\theta_c)\big\}$$

$$N = -\frac{2}{R_d^2}\Big\{[Z_{02b}\csc\theta_b(R_{2b}-1) - Z_{02c}\csc\theta_c(R_{2c}-1)]^2 + [R_{2b}Z_{02b}\cot\theta_b - R_{2c}Z_{02c}\cot\theta_c] \cdot \Big[Z_{02b}\cot\theta_b(2-R_{2b}) - Z_{02c}\cot\theta_c(2-R_{2c}) + \frac{1}{2}R_{2c}Z_{01b}\cot\theta_b\Big]\Big\}$$

and

$$M = -\frac{1}{R_d^2}(2M_1M_4 + M_2M_3) \tag{24}$$

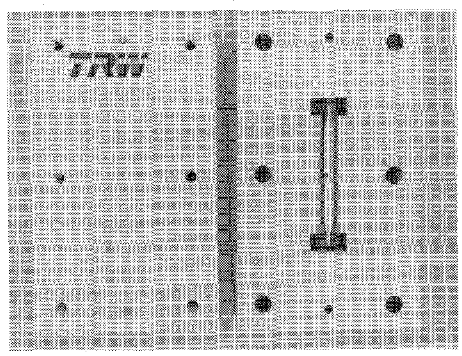

Fig. 8. Photograph of the two-line spurline filter.

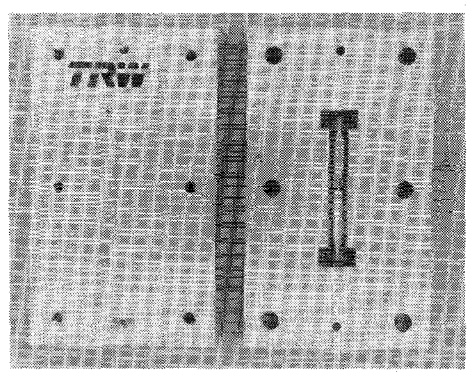

Fig. 9. Photograph of the three-line spurline filter.

with

$$\begin{aligned} M_1 &= Z_{02b}\cot\theta_b(1-R_{2b}) - Z_{02c}\cot\theta_c(1-R_{2c}) \\ M_2 &= 2Z_{02b}\cot\theta_b - 2Z_{02c}\cot\theta_c + R_{2c}Z_{01b}\cot\theta_b \\ M_3 &= R_{2b}Z_{02b}\csc\theta_b - R_{2c}Z_{02c}\csc\theta_c \\ M_4 &= Z_{02b}\csc\theta_b - Z_{02c}\csc\theta_c. \end{aligned} \tag{25}$$

V. Experimental Results

To validate the theory of spurline bandstop filters developed, single-section spurline bandstop filters with stopbands centered near 33 GHz were designed using suspended stripline and tested. To minimize the discontinuity and obtain a very compact structure, these filters have been fabricated within the width of a 50-Ω transmission line. The mode-characteristic impedances and mode-propagation velocities for the coupled lines are obtained numerically first. The theoretical characteristics of the test circuits have been calculated through the use of chain matrices. The responses of these filters are shown in Figs. 6 and 7. It can be seen that there is good agreement between calculated and measured responses. Figs. 8 and 9 are photographs of these filters. As shown in their photographs, these filters are connected to the 50-Ω input and output transmission lines.

VI. Conclusions

The results for the parameters of general two-coupled lossless lines and symmetrical three-coupled lossless lines embedded in an inhomogeneous medium have been obtained. By applying the appropriate port-termination conditions, the chain and impedance matrices of the corresponding spurline bandstop filters have been derived. The experimental results obtained on two- and three-conductor spurline bandstop filters were found to be in good agreement with the computed results. The results obtained should be useful in designing spurline bandstop filters in an inhomogeneous medium (homogeneous medium is a special case).

References

[1] R. N. Bates, "Design of microstrip spurline bandstop filters," *IEE J. Microwaves, Optics and Acoustics*, vol. 1, no. 6, pp. 209–214, Nov. 1977.

[2] B. M. Schiffman and G. L. Matthaei, "Exact design of bandstop microwave filters," *IEEE Trans. Microwave Theory Tech.*, vol. MTT-12, pp. 6–15, Jan. 1964.

[3] C. Nguyen, C. Hsieh, and D. Ball, "Millimeter wave printed circuit spurline filters," in *IEEE 1983 MTT-S Int. Microwave Symposium Dig.*, pp. 98–100.

[4] V. K. Tripathi, "Equivalent circuits and characteristics of inhomogeneous nonsymmetrical coupled-line two-port circuits," *IEEE Trans. Microwave Theory Tech.*, vol. MTT-25, pp. 140–142, Feb. 1977.

[5] V. K. Tripathi, "Asymmetric coupled transmission lines in an inhomogeneous medium," *IEEE Trans. Microwave Theory Tech.*, vol. MTT-23, pp. 734–739, Sept. 1975.

[6] V. K. Tripathi, "On the analysis of symmetrical three-line microstrip circuits," *IEEE Trans. Microwave Theory Tech.*, vol. MTT-25, pp. 726–729, Sept. 1977.

Cam Nguyen (S'82–M'83) received the B.S. degree in mathematics from University of Saigon, Vietnam in 1975, the B.S.E.E. from Cal Poly University at Pomona, and the M.S.E.E. from California State University at Northridge in 1979 and 1982, respectively. Presently, he is pursuing a Ph.D degree at USC.

In 1979, he joined ITT Gilfillan in Van Nuys, CA, and was involved in the design and development of various microwave components. From 1982 to 1983, he was employed by Hughes Aircraft Company, Torrance, CA, where he was responsible for the development of millimeter-wave mixers, upconverters, and filters. Since November 1983, he has worked at TRW Electronics and Defense, Redondo Beach, CA, where he is currently involved in the research and development of state-of-the-art millimeter-wave integrated-circuit components up to 170 GHz.

Mr. Nguyen is a member of Sigma Xi.

Kai Chang (S'75–M'76–SM'85) was born in Canton, China, on April 27, 1948. He received the B.S.E.E. degree from National Taiwan University, Taipei, Taiwan, the M.S. degree from the State University of New York at Stony Brook, and the Ph.D. degree from the University of Michigan, Ann Arbor, in 1970, 1972, and 1976, respectively.

From 1972 to 1976, he worked for the Microwave Solid-State Circuits Group, Cooley Electronics Laboratory of the University of Michigan as a Research Assistant. From 1976 to 1978, he was employed by Shared Applications, Ann Arbor, where he worked in microwave circuits, microwave radar detectors, and microwave tubes. From 1978 to 1981, he worked for the Electron Dynamic Division, Hughes Aircraft Company, Torrance, CA, where he was involved in the research and development of millimeter-wave devices and circuits. This activity resulted in a state-of-the-art IMPATT oscillator and power combiner performance at 94, 140, and 217 GHz. Other activities included silicon and gallium arsenide IMPATT diode design and computer simulation, Gunn oscillator development, and monopulse comparator and phase shifter development. In May 1981, he joined TRW Electronics and Defense, Redondo Beach, CA, as a Section Head in the Millimeter Wave Technology Department, developing state-of-the-art millimeter-wave integrated circuits and subsystems. In August 1985, he joined the Electrical Engineering Department of Texas A&M University as an Associate Professor.